Microporous and Mesoporous Materials 252 (2017) 17–28

Contents lists available at ScienceDirect

Microporous and Mesoporous Materials

journal homepage: www.elsevier.com/locate/micromeso

Adsorption of acetic acid and methanol on H-Beta zeolite: An experimental and theoretical study

Glaucio J. Gomes [a, c], M. Fernanda Zalazar [a, b, *], Cleber A. Lindino [c, **], Fernando R. Scremin [d], Paulo R.S. Bittencourt [d], Michelle Budke Costa [d], Nélida M. Peruchena [a, b]

[a] Laboratorio de Estructura Molecular y Propiedades, Facultad de Ciencias Exactas, Naturales y Agrimensura, Universidad Nacional del Nordeste (UNNE), Avenida. Libertad 5460, 3400 Corrientes, Argentina
[b] Instituto de Química Básica y Aplicada del Nordeste Argentino, IQUIBA-NEA, UNNE-CONICET, Avenida Libertad 5460, 3400 Corrientes, Argentina
[c] Grupo Interdisciplinar de Pesquisa em Fotoquímica e Eletroquímica Ambiental, Universidade Estadual do Oeste do Paraná (UNIOESTE), Rua da Faculdade 645, 85903-000 Toledo, Brazil
[d] Laboratório de Análise Térmica e Espectroscopia de Combustíveis e Materiais, Universidade Tecnológica Federal do Paraná (UTFPR), Avenida Brasil 4232, 85884-000 Medianeira, Brazil

ARTICLE INFO

Article history:
Received 29 March 2017
Received in revised form
23 May 2017
Accepted 5 June 2017
Available online 7 June 2017

Keywords:
Heterogeneous catalysis
DFT
Brønsted acid site
Combined TGA-IR
Green chemistry
Vibrational spectroscopy
ATR-FTIR
Zeolites

ABSTRACT

The adsorption of acetic acid and methanol on H-Beta zeolite as a model of reaction of first step of the esterification reaction has been investigated with TGA-IR coupled, ATR-FTIR spectroscopy together with Density Functional Theory (DFT) calculations at M06–2X/6-31G(D) level. From the theoretical viewpoint, different models of adsorption of acetic acid and methanol on the surface of H-Beta zeolite are studied. TGA-IR experiments show that both reactants are molecularly adsorbed on H-Beta, beyond 200 °C for methanol and 250 °C for acetic acid other species are also formed due to the surface reactivity being strongly adsorbed on the catalyst. Results from ATR-FTIR spectroscopy and theoretical calculations reveal that the predominant adsorption mode of acetic acid involves the ads_AA(C=O) complex where the acetic acid is molecularly adsorbed by the carbonyl group on the Brønsted acid site of catalyst, and the OH group is oriented to the Al-O-Si bridge. The mechanism of adsorption of both acetic acid and methanol is also discussed at molecular level. The complexes where the acetic acid is adsorbed by the carbonyl group are clearly the most stable one.

1. Introduction

The high dependence of non-renewable energies in several sectors, such as industry, transport and agriculture, generates growing concerns regarding the petrochemical market and climate change. In this context, biomass use for the production of modern bioenergy and biomaterials has grown significantly in order to oppose the depletion of fossil resources and to reduce greenhouse gas emissions [1].

Selective transformation of renewable biomass-derived feedstocks plays a key role in sustainable production of biofuels and fine chemicals [2]. In this context, esterification of carboxylic acids catalyzed by solid acid catalysts is a very important process in organic synthesis [3] as well as in the fuel industry, resulting in a promising alternative route for the use of free fatty acids (FFA) and bio-oils in esterification reactions, as promising candidates to replace petroleum fuels [4–7]. Different heterogeneous catalysts have been tested in the esterification of carboxylic acids and alcohols, including zeolites [8–11]. On solid acid catalyst type of zeolites, one might expect a similar esterification behavior to that of homogeneous catalysis; however, little is known about the reaction pathway.

* Corresponding author. Laboratorio de Estructura Molecular y Propiedades, Facultad de Ciencias Exactas, Naturales y Agrimensura, Universidad Nacional del Nordeste (UNNE), Avenida. Libertad 5460, (3400) Corrientes, Argentina
** Corresponding author. Grupo Interdisciplinar de Pesquisa em Fotoquímica e Eletroquímica Ambiental, Universidade Estadual do Oeste do Paraná (UNIOESTE), Rua da Faculdade 645, (85903-000) Toledo, Brazil
E-mail addresses: mfzalazar@conicet.gov.ar (M.F. Zalazar), lindino99@gmail.com (C.A. Lindino).

http://dx.doi.org/10.1016/j.micromeso.2017.06.008
1387-1811/

Zeolites are microporous aluminosilicate minerals that are widely used in industry as solid acid/base catalysts, and they have a network of cavities and channels of molecular dimensions. Zeolites are framework silicates consisting of interlocking SiO_4 and AlO_4 tetrahedrons, where the presence of tetrahedral Al in their chemical structure gives rise to very high acidic properties and constitutes what is known as acidic zeolites. Because of their high selectivity, reactivity and the presence of Brønsted acid sites (BAS), acidic zeolites act as catalysts in a variety of industrial processes [12].

Considering the diversity of zeolites available, only few acidic zeolites (H-BEA, H-ZSM5, H-MOR, HY etc.) have been tested as catalysts for esterification reactions of FFA to produce fatty acid methyl esters (FAME) or conversion of biomass and its derivatives from several different raw materials such as palm oil, soybean oil [13], oleic acid [14–17], among others [8,10,18,19].

Some authors suggest that zeolites with micropores are not suitable for production of FAME because micropores limit the diffusion of large molecules or because the formation of the transition states only takes place in zeolites that present large cavities [10,18,20]. Additionally, low reaction rate of esterification and low selectivity to products have been attributed to strong acid sites on H-ZSM-5 and H-FER zeolites, and strong adsorption properties of reactants [21]. By contrast, others authors suggest that pore mouth size and size of the cavity of the catalyst are not the main limiting factors for the reaction because good yields are obtained for both H-ZSM5 as well as H-MOR [13,14,16,22]. Other factors such as porosity and surface hydrophobicity of the catalyst, steric effects, acid strength, among others, have been reported to play a key role in the process [21,23,24].

Although the mechanisms of esterification of acids catalyzed by homogeneous catalysts are well established, the mechanisms of esterification catalyzed by heterogeneous catalysts are still debated, and specifically in acidic zeolites because of the complexity of the system catalyst-reactants. Specifically on zeolites, both Eley-Rideal (ER) and two-site mechanisms have been postulated for esterification. Koster et al. reported that esterification of acetic acid (AA) with ethanol over MCM-41 zeolite proceeds via a protonated AA intermediate and follows a Langmuir–Hinshelwood pathway [25]. In a related study, Kirumakki and co-workers also studied esterification of acetic acid with alcohols using H-BEA, H-FAU, and H-ZSM5 zeolites, and concluded that ester formation occurs via an Eley-Rideal pathway by which an activated acetic acid molecule reacts with alcohol in the bulk phase to form the corresponding acetate [26]. Both mechanisms involved a first step of acetic acid adsorption.

Recently, Bedard and co-workers [23] reviewed different mechanisms found in the literature and from their research made a new contribution to the topic. They studied the kinetics for AA esterification with ethanol on H-zeolites using kinetic measurements, and they proposed a mechanism that proceeds through a surface acetic acid/ethanol co-adsorbed complex. Thus, this mechanism involve two pathways of adsorption of the reactants on the zeolite surface.

In acid-catalyzed reactions, adsorption is the first step that initiates the reaction, and specifically in esterification reactions on zeolites, it has been suggested that both AA and alcohol adsorption are involved in the rate-determining reaction step [23]. According to these authors, the ability to discriminate the effects of zeolite structure on the kinetics of acid catalyzed reactions occurring in their constrained environments depends critically on dissecting chemical reactions into their elementary steps [23]. As a result, an elaborate understanding of adsorption mechanism of AA and methanol (MeOH) inside zeolite is prerequisite in order to shed light on the catalytic mechanism. Then, a thorough investigation of adsorption complexes is necessary in order to provide a better understanding of these acid catalyzed reactions that involve polar compounds and zeolites. A detailed scheme tying together different elementary steps of adsorption according to the different postulated mechanisms in the literature: Langmuir-Hinshelwood [25], Eley-Rideal [26], or a co-adsorbed complex [23] is shown in Scheme 1.

In an attempt to extend the knowledge about the course of these chemical reactions and as a result of the complexity of the reaction path, we found it interesting to study the elementary steps (including adsorption processes) of this chemical reaction in order to explain, at the molecular level, the complete mechanism and the stability of adsorbed intermediates. In this context, computational methods can be applied to gain new and useful molecular insights into adsorption mechanisms [27]. Furthermore, generation of fundamental knowledge at the molecular level is of paramount importance [28]. In previous works, by drawing on Density Functional Theory (DFT), we studied the adsorption of alkenes on acidic zeolites [29] and the alkene protonation reaction over acidic zeolites [30–32], thus providing a better understanding of the details of the electron redistribution upon these physical and chemical transformations.

In the present work, we study the adsorption of acetic acid and methanol on H-Beta as a model of reaction of the first step of esterification of FFA on H-zeolites. Understanding the adsorption model of both reactants is helpful to predict the different reaction pathways. We combined results from Thermogravimetric analysis coupled with Infrared spectroscopy (TGA-IR), Attenuated Total Reflectance-Fourier Transform Infrared (ATR-FTIR) spectroscopy, and quantum chemical methods in order to obtain an understanding, at the molecular level, of the interaction between model compounds of FFA with H-Beta zeolite. From the theoretical viewpoint, we study different models of adsorption and co-adsorption of AA and MeOH on the surface of H-Beta zeolite following the mechanisms proposed by Bedard et al. [23]. To the best of our knowledge, this is the first experimental and theoretical study that provides a profound analysis of the adsorption process of model compounds of FFA on H-Beta zeolite as the first step of solid catalyzed esterification reaction.

2. Experimental (methods and calculation details)

2.1. Reagents

Zeolite Beta (CP814C, BEA, $SiO_2/Al_2O_3 = 38$) in its ammonium form (NH_4^+Beta) was obtained from Zeolyst International. The reagents MeOH (99% v/v) and AA (99% v/v), were purchased from Sigma-Aldrich. All the reagents of analytical grade were used without further purification.

2.2. Preparation and characterization of the zeolite catalyst

The zeolites sample was submitted to thermal decomposition NH_4^+ to $NH_{3(g)}$ and H^+ by a PerkinElmer STA 6000 Thermo-Analyzer coupled with a PerkinElmer Infrared spectrometer by increasing the temperature from room temperature to 500 °C for 4 h under N_2 flow of 20 mL min^{-1} to obtain the protonated H-Beta. The textural and chemical characterization of these materials was accomplished by ATR-FTIR, using a PerkinElmer Spectrum 100 s Spectrometer. FTIR was obtained by the KBr wafer technique. N_2 adsorption and desorption measurements were carried out at −196 °C, using a Quantachrome Nova-1200 gas sorption analyzer. Prior to the analysis, the sample was pretreated at 150 °C under vacuum for 3 h. The surface area was estimated by the BET equation, using p/

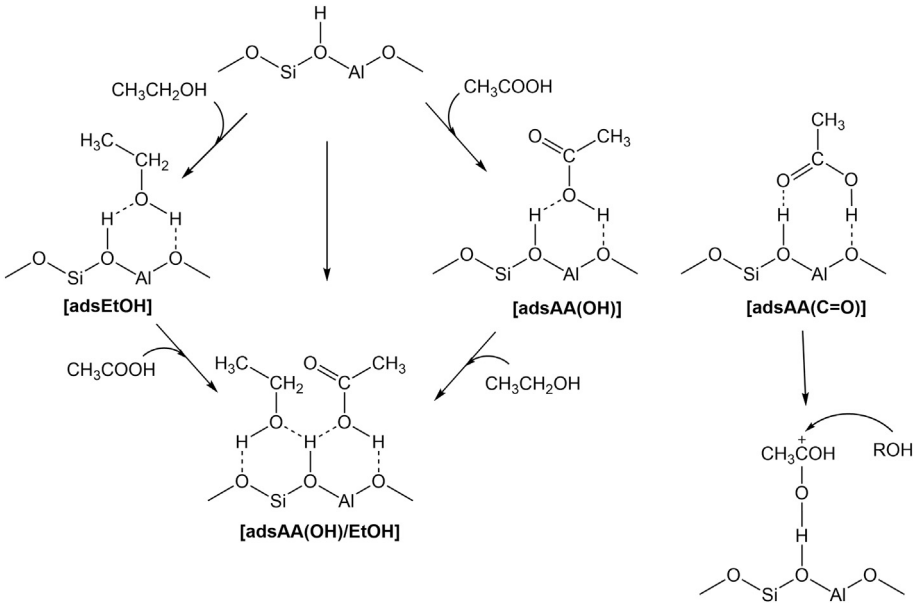

Scheme 1. Combined overview of different elementary steps of adsorption involved on the esterification of AA by alcohols over H-zeolites according to different postulated mechanisms in the literature: Langmuir-Hinshelwood [25], Eley-Rideal [26], or a co-adsorbed complex [23]. adsEtOH: first step of alcohol adsorption; adsAAOH: first step of acetic acid adsorption by OH group; adsAA(OH)/Et(OH): co-adsorbed complex postulated by Bedard [23]; adsAA(C=O): first step of acetic acid adsorption by C=O group followed by activation of acetic acid to form a surface acetyl and subsequent reaction with an alcohol [26].

$p_0 \leq 0.3$ [33]. These data have been reported in the supplementary information section.

2.3. Isothermal process

The isothermal process of AA and MeOH over H-Beta was studied by TGA-IR. A sample of 20 mg of catalyst was packed into a platinum crucible and flushed at 500 °C for 1 h with N_2 at a flow rate of 20 mL min^{-1}. After pretreatment, the temperature was reduced to 50 °C and 100 μL of MeOH and AA were placed into a platinum crucible. The AA and MeOH were added in excess to ensure saturation of the entire acid site in the catalyst. After AA and MeOH adsorption onto the catalyst, nitrogen carrier gas was flushed over the bed at a rate of 20 mL min^{-1} from 50 to 100 °C for 1 h to remove excess adsorbed reagents. After the isothermal process, the samples are stabilized at 50 °C and then heated to 665 °C at a heating rate of 10 °C min^{-1}. The products desorbing from the catalytic surface during the temperature ramp were analyzed by IR. The transfer line was heated and maintained at an internal temperature of 240 °C to avoid condensation or adsorption of semi-volatile products during the thermal degradation process. The IR spectrum was recorded every 9 s in the spectral range between 4000 and 650 cm^{-1} with a resolution factor of 2 cm^{-1}. There is an approximate 100 s delay between the TGA result and the corresponding spectra.

2.4. In situ ATR-FTIR spectroscopy

Infrared spectroscopic study of AA and MeOH adsorption on H-Beta was conducted in ATR-FTIR mode using a diamond crystal. After the zeolite was pretreated at 500 °C in TGA-IR with N_2 flow of 20 mL min^{-1} for 1 h, the temperature was reduced to 70 °C and a blank spectrum of the zeolite surface was taken as reference. The reagents were then adsorbed onto the surface for 50 min at 105 °C for AA and at 55 °C for MeOH to remove the excess of adsorbed reagents on the zeolite surface. After the thermal treatment, the samples of adsorbed reagents on zeolite were heated to 150 °C for AA and to 100 °C for MeOH for spectra collection. The spectra were acquired in the range of 4000–600 cm^{-1} at a resolution of 2 cm^{-1}.

2.5. Quantum chemical calculations

Coordinates of the BEA zeolite framework were obtained from the International Zeolite Association online database [34]. The zeolite catalyst has been modeled by a 52T (T = Si and Al tetrahedral sites) quantum cluster model, with an overall composition $H_{62}O_{72}Si_{51}Al(OH)$. (see Fig. S1 of the supporting information). This extended cluster include the cavity that emerged at the channels intersection of the catalyst and, therefore local effects (interaction of adsorbates with the Brønsted and Lewis acid sites) and nonlocal effects (van der Waals interactions with the zeolite cavity or confinement effects) are taken into account. The active site was positioned at the intersection channel because these locations offer maximal available space, result in minimal restrictions and has been chosen as the active site for the study of several reactions [35–38]. Similar 52T cluster model was used by Van der Mynsbrugge and co-workers for the study of benzene methylation by methanol on H-Beta zeolite [37].

Initially, because the system is computationally demanding, we used a combined theoretical model, namely ONIOM [M06–2X/6-31G(D):PM6], in order to predict the geometries of various adsorption structures (results not shown). To preserve the integrity of the zeolite structure during the structure optimizations, only the acid site region ($AlOHSi_2O_9$ or 3T) and the adsorbed molecule in the high-level layer were relaxed while the rest of the system was fixed. The most stable structures were selected and re-optimized using Density Functional Theory. During geometry optimization, all atoms of the 52T zeolite cluster model were frozen in their optimized position except for atoms located in the 3T region and the reactant molecules. The M06–2X [39,40] density functional and the 6-31G(D) basis set were used in all calculations. Previous studies by others authors showed that the density functional theory using the M06–2X functional provided quite good results compared to functionals without dispersion energy terms for study the

interaction of organic molecules inside the zeolite pores, including polar molecules [40–45].

All stationary points were characterized by calculating the Hessian matrix and analyzing the vibrational normal modes. Vibrational frequencies were scaled by the factor 0.947 [46]. From each optimized geometry, vibrational modes were used to obtain zero-point vibrational energies and finite temperature corrections required to calculate enthalpies. All calculations were performed with the Gaussian 09 software [47].

The adsorption (E_{ads}) and co-adsorption energies ($E_{co\text{-}ads}$) for stepwise process were calculated by:

$$E_{\text{ads}} = E_{(\text{adsorbed complex})} - \left[E_{(\text{zeolite})} + E_{(\text{reactant1})}\right] \quad (1)$$

$$E_{\text{co-ads}} = E_{(\text{co-adsorbed complex})} - \left[E_{(\text{adsorbed complex})} + E_{(\text{reactant2})}\right] \quad (2)$$

where $E_{(\text{adsorbed complex})}$ is the total energy of optimized adsorbed complex, $E_{(\text{zeolite})}$ the total energy of the H-Beta zeolite, $E_{(\text{reactant})}$ the total energy of the isolated reactant molecule (MeOH or AA) and $E_{(\text{co-adsorbed complex})}$ the total energy of optimized co-adsorbed complex.

For concerted process, the adsorption energy was calculated via Equation (3).

$$E_{\text{ads}} = E_{(\text{adsorbed complex})} - \left[E_{(\text{zeolite})} + E_{(\text{reactant1})} + E_{(\text{reactant2})}\right] \quad (3)$$

3. Results and discussion

3.1. Characterization of catalysts

Activation of the H-Beta zeolite was performed by combined TGA-IR, resulting in the identification of two mass loss processes (see Fig. S2 of the supporting information). The first process identified by Derivative Thermogravimetric Analysis (DTG) is related to the desorption of water molecules that are free or adsorbed on the surface of the zeolite. It occurs between 50 and 250 °C, and similar results were found by other authors for other zeolites [48,49]. A new process relative to the thermal degradation of NH_4^+ occurred from 270 °C to 580 °C, as shown by IR in the analysis of desorbed gases of the zeolite (Fig. S3 of the supporting information).

The spectra of the desorbed gases of the catalyst in the region of 1200–700 cm^{-1}, as a function of the temperature variation (50–665 °C), present two bands in the regions of 963 cm^{-1} and 929 cm^{-1}, referring to the desorption of NH_3 on the surface of the catalyst, according to the previous study by Hippler and co-workers [50]. This thermal process results in the formation of Brønsted acid sites, since NH_3 molecules do not exhibit high adsorption affinity on Lewis sites that are unable to form strong hydrogen bonds, resulting in the formation of active sites on the zeolite, this effect is in agreement with the results of other authors [51]. The surface area found for the H-Beta zeolite was 571 $m^2\ g^{-1}$, similar to previous findings in the literature [23]. The experimental IR-spectrum of H-Beta is characterized by a band in the 3615–3600 cm^{-1} interval corresponding to the isolated BAS, and another in the 3750–3740 cm^{-1} range associated with external silanol groups [52,53]. The FTIR identified the presence of framework Si–OH–Al groups at 3640 cm^{-1}, water at 3442 cm^{-1} and 1628 cm^{-1} (supporting information, Fig. S5 and Table S2). ATR-FTIR identified the presence of silanols groups at 3740 cm^{-1} (Fig. S6 of the supporting information) according to results reported previously by Bordiga et al. [52].

3.2. Acid acetic and methanol adsorption by using TGA-IR

The adsorption of AA and MeOH was previously studied on the desorption isotherm as shown by the supporting material Fig. S7. In this process, 70% of mass of AA at 115 °C and of MeOH at 55 °C were removed, in which both experiments were stabilized between 25 and 30 min. Removal of excess of AA and MeOH in the isotherm is associated with molecules of both reactants that are adsorbed in layers or do not interact with silane groups (≡Si-OH) or with Brønsted acid sites of the H-Beta zeolite. The desorption process of the adsorbed molecules on the catalyst after the isothermal process was monitored by TGA-IR. The thermogravimetric profile of the desorption of AA and MeOH under inert atmosphere (N_2) is shown in Fig. 1. Then, the IR spectra of the desorbed gases from the catalyst surface were also monitored, as shown in Fig. 2.

3.2.1. Thermogravimetric - evolved gas analysis for MeOH

The results concerning the TGA curve show mass loss that ranges from 50 °C to 665 °C (Fig. 1a). The analysis of DTG for MeOH desorption showed four interconnected processes. The first two processes (identified by the convolution peaks at 95 °C and 142 °C) occur between 50 and 206 °C and are relative to MeOH molecules physisorbed on the surface of H-Beta. Other authors using ZSM-5 zeolite suggested that during the desorption/reaction process most of the protonated methanol is desorbed without reacting below 226–249 °C [54,55] similar behavior is observed in this work.

The gases desorbed from the catalyst surface were monitored by IR, as shown in Fig. 2a. For the desorption of MeOH in the gas phase, there were bands at 2972 cm^{-1} for the axial deformation of the C-H bond and 1053 cm^{-1} for deformation of the C-O bond present in MeOH molecules desorbed in the gas phase. Above 210 °C, no free MeOH spectra were identified. However, the spectrum identified that the band in the region of 2972 cm^{-1} extends to 300 °C, referring to symmetrical and asymmetrical stretching Csp3-H [56] that are related to a species desorbed from the surface of the catalyst. The hypothesis for the interpretation of this effect is centered on decomposition of hydrocarbon species (HC) resulting from the reactivity of methyl groups covalently adsorbed on the surface of the zeolite (Al-O-CH_3) suggesting the presence of dimethyl ether and HC species as was suggested by other authors [57]. Mirth and Lercher, when investigating the surface chemistry of methanol on H-ZSM-5, also suggested, the formation of dimethyl ether and HC molecules that are produced by the reactivity of methanol with methoxides [SiO(CH_3)Al] [54]. The third and fourth processes between 240 °C and 303 °C are attributed to the thermal degradation of Al-O-CH_3, resulting in the deactivation of the catalyst.

3.2.2. Thermogravimetric - evolved gas analysis for AA

The results of the desorption of AA by TGA show a 10% mass loss over a wide temperature range (50–565 °C), which starts above 100 °C. Based on the deconvolution of the DTG curves, four different mass loss processes could be identified.

The first process at 175 °C refers to the desorption of AA molecules that are physically adsorbed on ≡Si-OH groups and Brønsted acid sites by hydrogen interactions, forming a desorption temperature range that starts above 90 °C and extends to 250 °C. Similar results were reported by other authors for H-ZSM-5 [58]. The desorbed gases of the surface up to 250 °C confirmed the desorption of AA monomers monitored by the evolution of the bands at 1798 cm^{-1} and 1772 cm^{-1}, relative to the axial deformation of C=O, and 1179 cm^{-1}, relative to the deformation of the C=O stretching. Phung et al. for AA adsorbed on alumina catalyst showed that the gas phase spectrum of AA is composed by the spectra of the

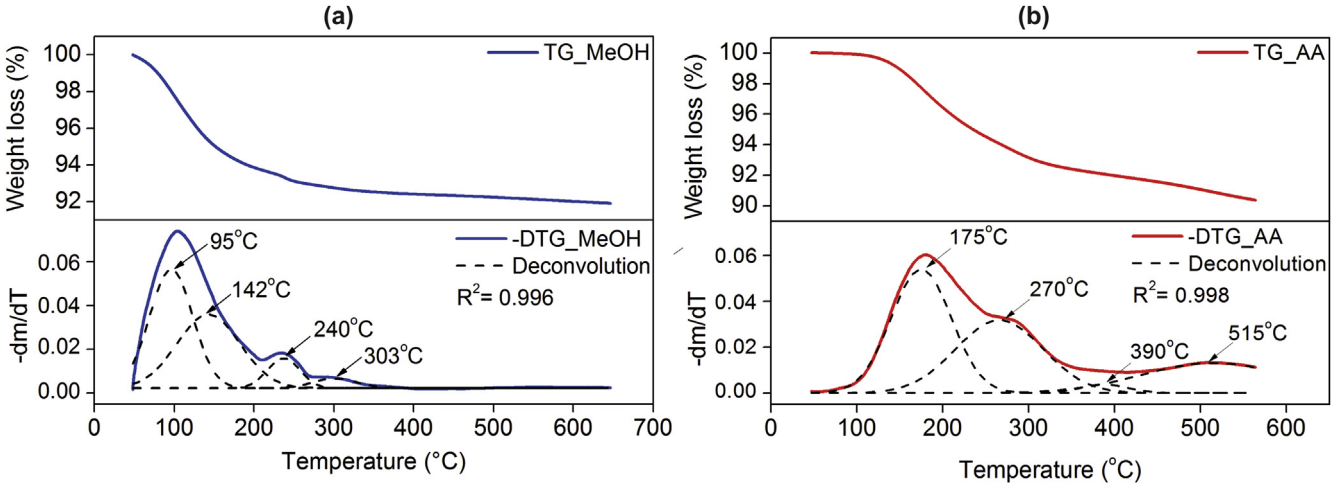

Fig. 1. Thermogravimetric Analysis (TGA), Derivative Thermogravimetric Analysis (DTG) and deconvolution of the DTG curves results for (a) adsorption of methanol on H-Beta (b) adsorption of acetic acid on H-Beta. Conditions: N_2 flow 20 mL min^{-1}; Temperature range from 50 to 650 °C with a heating rate of 10° C min^{-1}.

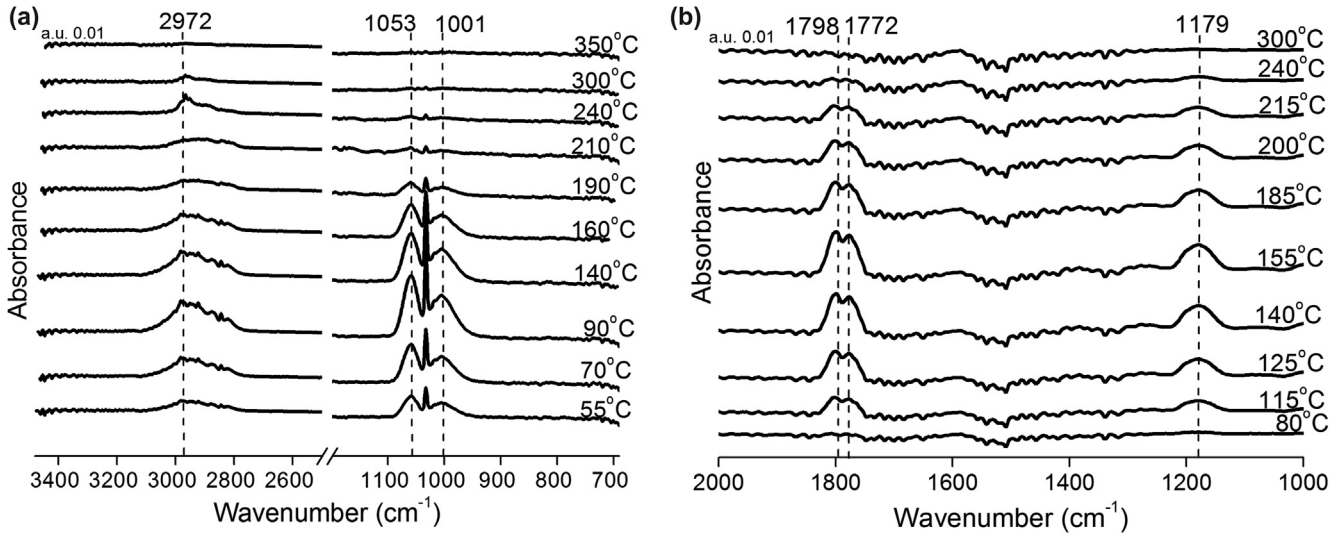

Fig. 2. IR spectra of desorbed gas phase of (a) methanol and (b) acetic acid adsorbed on H-Beta zeolite.

monomeric species (C═O stretching mode at 1788 cm^{-1}), and the H-bonded dimer (C═O stretching at 1729 cm^{-1}), the spectrum is essentially not modified until 250 °C [59].

The second process at 270 °C is directly interconnected with the reactivity of AA over BAS, because in this process the presence of free AA is not identified by IR. The findings indicate that the formation of a strongly adsorbed species possibly occurred on the acid zeolite, and this species is degraded above 270 °C. Previous studies by Kresnawahjuesa et al. on the desorption of AA in HZSM-5, monitored by mass spectrometry and gas chromatography, identified the formation of products such as CO_2 and acetone between 226 °C and 326 °C [58]. Thus, the effects found by TGA-IR indicate that the first and second processes are interconnected and the mass loss of DTG above 270° refer to the thermal degradation of adsorbed AA onto the zeolite structure as an intermediate. The gradual increase in temperature causes simultaneous reactions that result in the formation of acetone, water, ethylene, methane and CO_2 as products desorbed on the zeolite surface [58,60].

The third process identified by DTG deconvolution at 390 °C characterizes the desorption of a small amount of carbon resulting from the formation of high molecular weight species on the catalyst, thus initiating the fourth process, identified at 515 °C, in which there occurs the oligomerization and condensation of high molecular weight HC species that are degraded on the surface of the catalyst at high temperatures, deactivating the catalytic sites because of coke formation on the catalyst.

The behavior of both reagents (AA and MeOH) adsorbed on H-Beta were observed by deconvolution of the DTG curves (Fig. 1). The observations show that, in both desorptions and readsorption process, the values of the deconvolution peak above 100 °C can be affected by several factors as demonstrated by Gorte, informing that in many cases, only qualitative features can be obtained [61]. The results from DTG suggest that the first molecules to be desorbed are interacting with ≡ Si-OH groups or with adsorbed molecules on BAS. Then, the desorbed molecules result from the adsorbed molecules on the Brønsted sites inside the zeolite resulting in stronger interactions (hydrogen bonding) in which both the acidic strength of the BAS and the confinement effect of the framework of catalyst favour a strong adsorbate-catalyst interaction.

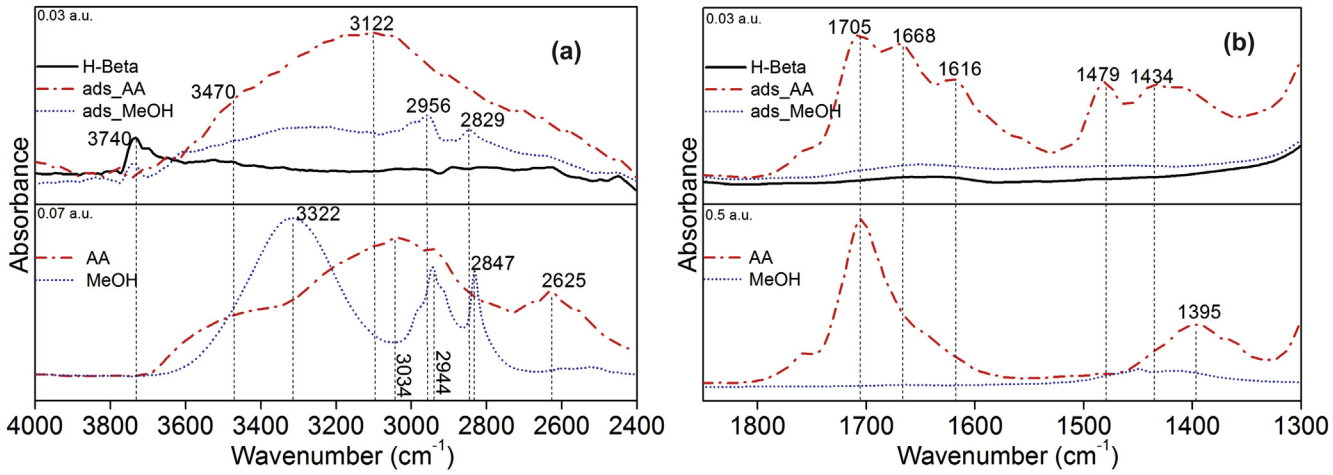

Fig. 3. ATR-FTIR spectra in the region of (a) 3800-2400 cm^{-1} and (b) 1900-1300 cm^{-1}. Top panel: H-Beta zeolite (black solid line), adsorbed methanol (blue dotted line) and adsorbed acetic acid (red dashed line) on H-Beta zeolite. Down panel: acetic acid and methanol. (For interpretation of the references to colour in this figure legend, the reader is referred to the web version of this article.)

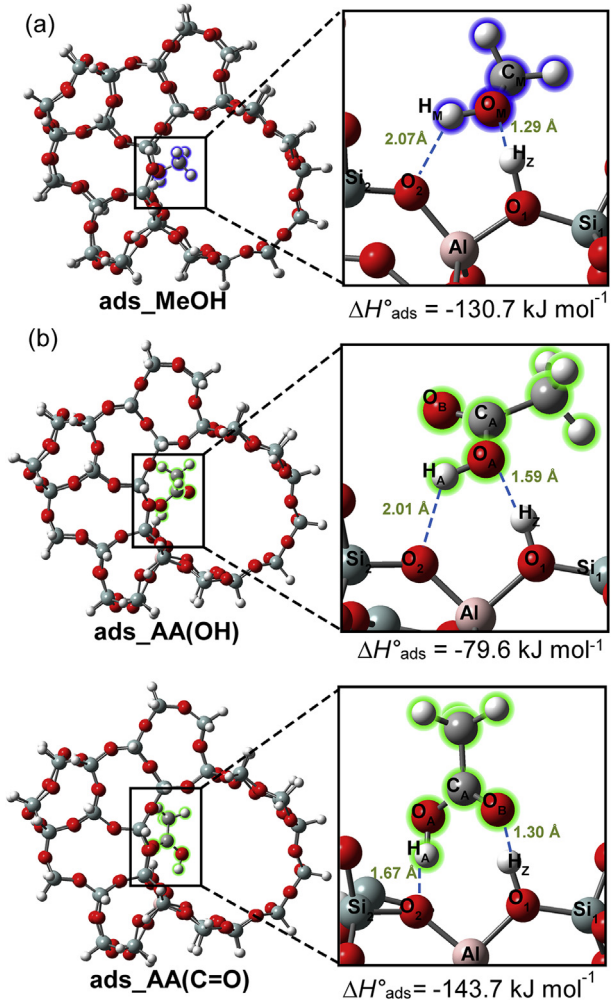

Fig. 4. Most stable structures found for the adsorption of acetic acid and methanol on the Brønsted acid site of H-Beta zeolite: (a) Adsorbed methanol; (b) Adsorbed acetic acid where ads_AA(C═O) involves the adsorption of the AA on the BAS by the carbonyl group and ads_AA(OH) implied the adsorption of the AA on BAS by the hydroxyl group.

3.3. In situ ATR-FTIR spectroscopy and quantum chemical calculations

The ATR-FTIR spectra of MeOH and AA adsorption on H-Beta zeolite are shown in Fig. 3. Fig. 4 shows the most stable structures found for adsorbed MeOH and AA on H-Beta, and Table 1 reports their corresponding energies. Table 2 summarized the most important vibrational frequencies calculated at M06–2X/6-31G(D) level for the isolated molecules and the adsorbed complexes. Moreover, the same table also lists experimental and theoretical frequencies of AA recently published by other authors [62] in order to validate the methodology used in this work.

3.3.1. Methanol adsorption

Methanol adsorption inside zeolites is a research topic on which several studies, both experimental and theoretical, have been reported in the literature [27,53,63–71]. Our results are in general accord with the majority of previously published data and will be discussed only briefly.

The IR spectra of the gas phase alcohols is characterized by C–H stretching (3065–2902 cm^{-1}) and bending (1471–1422 cm^{-1}), CH_3 bending (1423–1345 cm^{-1}) and OH stretching (3787–3747 cm^{-1}) vibrations [64]. In the liquid phase, a broad band between the 3800-3100 cm^{-1} interval with a wavenumber at 3250 cm^{-1} is assigned to the hydrogen-bonded OH groups [72]. For methanol adsorbed in zeolites (H-MOR, H-Y and H-ZSM5), there have been reports of bands around 3000–2800 cm^{-1}, corresponding to CH stretching bands, around 1470–1380 cm^{-1} corresponding to CH bending, and at 3230 cm^{-1} related to adsorbed methanol dimer [66]. Additionally, a recently experimental and theoretical study of ethanol adsorption on H-ZSM-5 showed that ethanol adsorbs at low ethanol loading as a single monomer on BAS (characteristic band at 3550 cm^{-1}), and at higher ethanol loading as a predominant dimeric species (broad band around 3200 cm^{-1}, low intensity) [73].

Isolated methanol shows a strong band in the 3600–3100 cm^{-1} region centered at 3322 cm^{-1}, indicating the presence of hydrogen-bonded OH groups; also, the 2944 and 2832 cm^{-1} symmetrical and asymmetrical bands related to the C-H stretching are observed in the high wavenumber region (Fig. 3a). After the adsorption process, C–H bands decreases and shifts toward higher wavenumbers (around 2956 and 2847 cm^{-1}) and, *ν*OH band decreases drastically in intensity. The last observation is associated with the *(i)* hydrogen

Table 1
Adsorption energies (E_{ads}), adsorption energies corrected by ZPE ($E_{ads+zpe}$), adsorption enthalpies (ΔH°), and co-adsorption energies ($E_{co\text{-}ads}$), in (kJ mol^{-1}) for adsorption of methanol and acetic acid on H-Beta zeolite calculated at M06–2X/6-31G(d) level.

	Adsorption			Co-adsorption		
Adsorbed complex	E_{ads}	$E_{ads+zpe}$	ΔH°_{ads}	$E_{co\text{-}ads}$	$E_{co\text{-}ads+zpe}$	$\Delta H^{\circ}_{co\text{-}ads}$
Stepwise						
ads_MeOH	−119.7	−125.9	−130.7	–	–	–
ads_AA(C=O)	−128.2	−140.9	−143.7	–	–	–
ads_AA(OH)	−83.0	−80.6	−79.6	–	–	–
ads_AA(OH)-coads_MeOH	–	–	–	−81.3	−81.0	−86.5
ads_AA(C=O)-coads_MeOH	–	–	–	−59.1	−58.0	−60.8
ads_ MeOH-coads_ A(C=O)	–	–	–	−93.4	−91.3	−90.2
ads_ MeOH-coads_ AA(OH)	–	–	–	−74.1	−72.5	−65.0
Concerted						
ads_AA(C=O)/MeOH	−190.0	−188.7	−194.6	–	–	–
ads_AA(OH)/MeOH	−151.4	−150.3	−153.1	–	–	–

Table 2
Vibrational frequencies (cm^{-1}) for H-Beta zeolite, acetic acid (AA), methanol (MeOH) and adsorbed complexes[a] calculated at M06–2X/6–31(G) level.[b]

	AA[c]		H-Beta	AA	ads_AA(C=O)	ads_AA(OH)	MeOH	ads_MeOH
	Exp.	Calc.	Calculated					
$\nu(OH_z)$	–	–	3562	–	1269	2777	–	1477
ν(OH)	3564	3794	–	3578[d]	3070	3446	3636	3473
ν(C=O)	1779	1805	–	1818	1758	1845	–	–
ν(C-O)	1259	1353	–	1185	1267	1156	1077	1061
νHCH_2 s.	3051	3237	–	3051	3051	3056	3007	3057
νHCH_2 a.	2996	3196	–	3018	3006	3008	2933	3029
νCH_3	2944	3115	–	2946	2934	2940	2882	2944
δHCH_2 s.	1434	1501	–	1425	1409	1417	1464	1448
δHCH_2 a.	1439	1506	–	1425	1424	1414	1451	1451
δCH_3	1379	1434	–	1305	1336	1357	1435	1477

[a] Ads_AA(C=O): adsorption of acetic acid on the BAS by C=O group; ads_AA(OH): adsorption of acetic acid on the BAS by OH group; ads_MeOH: adsorption of methanol.
[b] All frequencies were scaled by a factor of 0.947 [46].
[c] From Ref. [62].
[d] For acetic acid dimer, ν(OH) = 3136 cm^{-1} (doubly H-bonded structure).

bonding interactions between adsorbed MeOH on BAS and molecules of MeOH that have been desorbed, *(ii)* the strong adsorption of MeOH on both BAS (H_z) and with a nearest-neighbor framework oxygen bridge with respect to the acid proton (O_2), leading to a decrease in intensity of νOH after adsorption. Then, our results show a physical adsorption of methanol on the surface of H-Beta zeolite, but not proton transfer.

For methanol adsorption on H-ZSM5, Lee and Gorte reported an experimental value of −115.5 kJ mol^{-1} [74], no experimental data for methanol adsorption on H-Beta are founded in the literature. The calculated adsorption energy (E_{ads}) for MeOH adsorption on H-Beta is −119.7 kJ mol^{-1} (See Table 1), which agrees with the calculated energy reported by other authors at the B3LYP-D3 level [37] and, is close to the experimental value reported for H-ZSM-5. The above mentioned papers have described the presence of two hydrogen-bonds: the first is medium to strong and the second is much weaker.

For H-Beta, our theoretical calculations predict the νOH_z stretching band at 3562 cm^{-1} (Table 2). For gas phase MeOH, the IR spectra shows the C–H stretching bands at 3007 cm^{-1} and 2993 cm^{-1} (symmetrical and asymmetrical respectively), C–H bending bands at 1464 and 1451 cm^{-1}, and OH stretching at 3636 cm^{-1}. Upon methanol physisorption, the frequencies related to νCH_3, δHCH_2 and δCH_3 are not significantly affected by complex formation. However, there was a slightly shift of νHCH_2 towards higher wavenumbers (shift from 2933 cm^{-1} to 3029 cm^{-1}), because of a hydrogen bonding with an oxygen atom (O_Z) of the framework. In addition, the νOH stretching mode is shifted to lower wavenumbers (3473 cm^{-1}) and the νOH_Z one is shifted to 1477 cm^{-1} ($\Delta\nu$ = 2085 cm^{-1}), showing a stronger adsorption in agreement with other authors [52,64,69].

3.3.2. Acetic acid adsorption

For AA adsorption, two possibilities for the interaction of the AA with the proton of the BAS (H_z) can be occur, that is, by interaction of the carbonyl or the hydroxyl group of the AA with the BAS, resulting in a different activation of the organic molecule. Both possibilities have been investigated, and the most stable structures found for adsorbed AA are shown in Fig. 4b.

It was found that the most stable structure for the adsorption of the AA corresponds to the ads_AA(C=O) complex, where the main interactions are $H_Z\cdots O_B$ (d = 1.30 Å) and $H_A\cdots O_2$ (d = 1.67 Å). The last one is related to the interaction between the hydroxyl group of AA and the oxygen of the Al-O-Si bridge (O_2) of the catalyst. The first one can be characterized as a strong hydrogen bond and the second as an H-bond of moderate strength according to geometrical parameters [75]. In addition, the methyl group lies near the intersection of both channels and its hydrogen atoms are oriented to the closest oxygen atoms of the framework of the catalyst (O_z) giving rise to possible H-Bond interactions.

For the ads_AA(OH) complex, the OH group of AA interacts with both Brønsted acid site and O_2, and the main interactions are $H_Z\cdots O_A$ (d = 1.59 Å), and $H_A\cdots O_2$ (d = 2.01 Å). In this case, the carbonyl oxygen (O_B) does not show a direct interaction with the acid or basic site.

The adsorption enthalpy for the ads_AA(C=O) complex (ΔH°_{ads} = −143.7 kJ mol^{-1}) is lower than that of the ads_AA(OH) complex (ΔH°_{ads} = −79.6 kJ mol^{-1}) by 64 kJ mol^{-1}. Other possible

adsorbed complexes are found to be higher in energy (results not shown). To the best of our knowledge, no data for adsorption energies of AA on H-Beta have been reported in the literature. In addition, Table 1 shows minor differences between corrected adsorption energies and adsorption enthalpies. The most stable complex involves a structure where the C=O group is oriented to the proton of the BAS and the OH group is oriented to the Al-O-Si bridge, forming two hydrogen bonds; in addition, the hydrogens of methyl group are oriented to the oxygen atoms of the zeolite wall. Then, the main difference is related to the orientation of the organic molecule in the cavity; as can be observed in the model ads_AA(C=O), the carboxylic group is oriented in order to promote stronger and more numerous adsorbate-catalyst interactions.

The ads_AA(C=O) complex is the most stable one probably because AA is oriented in order to form two strong hydrogen bonds between both oxygens (carbonyl and hydroxyl group) with the zeolite; by contrast, the ads_AA(OH) complex does not show any direct interaction between the carbonyl oxygen and the BAS or the Al-O-Si bridge.

Vibrational Assignments: before we have analyzed different adsorption configurations of AA, in the following we analyze the vibrational features of these configurations. Vibrational assignments of experimental infrared spectra have been made by comparing them with those previously reported in the literature for the FAU zeolite [76] and also with the computed ones. The assignment of experimental frequencies is based on the observed frequency shifts and the intensity changes in the infrared spectra of adsorbed species and, are confirmed by establishing a correlation between observed and theoretically calculated frequencies. In general, the frequencies of the experimental infrared spectra are quite nicely predicted by the calculation. As can be observed in Table 1, our calculated frequencies for isolated AA are in agreement with the experimental values and previously reported frequencies calculated at MP2/6−311++G(2d,2p) level [62]. In addition, it is interesting to emphasize that with ATR-FTIR spectroscopy, the analysis is based on the probe molecule.

The ATR-FTIR spectrum of AA pure in the 1900−1300 cm^{-1} region shows a band centered at 1705 cm^{-1} and another one centered at 1395 cm^{-1} (see Fig. 3b). The interpretation of the vibrational spectrum of adsorbed acetic acid on H-Beta zeolite, in the region of 1900−1300 cm^{-1}, is difficult because the spectrum reflects overlapping broad bands, hence the assignment of the observed bands is not straightforward and, in such situations, computational methods can be helpful.

Murphy and co-workers [76] studied the exchange of hydrogen between AA and the Na cation of NaY, and found the vibrational bands corresponding to the C=O stretching mode (νC=O, 1730 and 1707 cm^{-1}), and CH_3 bending modes [δCH_3, 1430 cm^{-1} (asymmetric) and 1385 cm^{-1} (symmetric)] of AA, indicating the presence of molecularly adsorbed AA (formed before the hydrogen/Na exchange). Kresnawahjuesa et al., by using FTIR spectroscopy, showed that AA forms a strong hydrogen-bonded complex with the Brønsted sites of H-ZSM5 zeolite that is characterized by ν(C−H) stretching frequencies of 1740 and 1750 cm^{-1} [58]. However, none of them reported a specific adsorption mode. In order to answer the critical question about the reaction mechanism and how the AA molecules are preferably oriented on the active site of the catalyst, an understanding of the adsorption mode should be provided, since the mode of adsorption of AA (either by OH or by C=O) will determine different paths in the next step of the reaction. Bedard et al. suggested in their proposed mechanism that the adsorption mode of AA should be by the OH group (according to their Scheme 4) [23].

After adsorption, the shift toward higher wavenumbers at 1434 cm^{-1} in the bending CH_3 region and the appearance of a new band at 1479 cm^{-1} may be attributed to the interaction between the hydrogens of the methyl group and the oxygen of the zeolite lattice. Nevertheless, there were no significant differences when comparing the shift of these calculated frequencies (δHCH_2 a./s. or δCH_3) between both AA adsorbed complexes [ads_AA(C=O) and ads_AA(OH)] and the free AA; thus, the analysis of these frequencies in both experimental and theoretical spectra does not indicate any evidence to discriminate between both adsorption modes (Table 2). In addition, the vibrational properties of adsorbed complexes are influenced by the interaction with the zeolite framework which, in turn, depends on its position within the zeolite.

Focusing the attention on the spectral region between 1800 and 1600 cm^{-1} (Fig. 3b), it can be seen that the νC=O band changes in relative intensity (decreases), and two new bands centered at 1668 and 1616 cm^{-1} appear, thus indicating that the acetic acid is molecularly adsorbed (but not protonated) and interactions between the carbonyl and the catalyst are presented (interactions that perturb the electronic density of carbonyl oxygen and weaken the double bond). However, one cannot distinguish which model prevails between the two adsorption models.

Similarly, in both adsorption modes the changes in calculated νC=O are similar (Table 2), but differences in ΔH°_{ads} are significant (Table 1). As can be seen, theoretical results do not differentiate adsorption mode only by analyzing the νC=O because it does not change significantly [shifted 27 cm^{-1} toward higher wavenumbers or shifted 60 cm^{-1} toward lower wavenumbers, for ads_AA(OH) and ads_AA(C=O), respectively].

In the 4000−2400 cm^{-1} region (Fig. 3a), the isolated acetic acid spectrum exhibits a band centered at 2625 cm^{-1} that is attributable to C-H stretching and, another extremely broad band in the 3700−2700 cm^{-1} region (higher intensity at 3034 cm^{-1}) which upon adsorption appears as a new broad band centered at 3122 cm^{-1}. In addition, the νOH band at 3740 cm^{-1} for isolated H-Beta catalyst disappears after adsorption, showing that AA was adsorbed not only on the Brønsted acid site, as well as on the external silanol groups (weak interaction).

For isolated AA, the signal at 3034 cm^{-1} band (Fig. 3a) is attributed to the acetic acid dimer due to the hydrogen-bonded structure [ν(OH) = 3136 cm^{-1}, Table 2]. After adsorption, an evident spectral perturbation is observed. An interesting discussion is showed by the analysis of the νOH stretching mode of AA from theoretical calculations. For adsorbed complexes, significant differences are observed when comparing the magnitudes of the ν(OH) in ads_AA(C=O) with ads_AA(OH). Results from theoretical calculations predict that for ads_AA(C=O) the band due to OH stretching mode of adsorbed acetic acid should be appear at approximately 3070 cm^{-1}, whereas if the adsorption mode is ads_AA(OH) then, ν(OH) should appear at 3446 cm^{-1} (See Table 2). In addition, no significant differences should be observed on $\Delta\nu$(C=O).

Then, the broad band centered at 3122 cm^{-1} is assigned to the OH stretching frequency in the ads_AA(C=O) complex according to the calculated frequencies. This vibrational frequency is associated with the OH stretching toward the Al-O-Si bridge, indicating that the adsorption mode of AA is related to the adsorption of the carbonyl group on the Brønsted acid site (See Fig. 4b). In summary, these results suggest that the predominant adsorption mode involves the ads_AA(C=O) complex.

3.3.3. Co-adsorption of acetic acid/methanol

Elementary steps of physical adsorption were considered in order to obtain the adsorbed complex of acetic acid/methanol postulated by Bedard [23]. We will restrict our discussion to the possible routes for formation of this complex because it has been

suggested that it is involved in the rate-determining reaction step of the mechanism of Bedard. The formation of this adsorbed complex on Brønsted acid site can originate from two separate pathways (by a stepwise or a concerted process) that will give rise to several different adsorption structures. The first option (stepwise process) involves the adsorption of AA and co-adsorption of MeOH where two different possibilities were analyzed; first, the adsorption of AA, where the adsorption on the BAS occurs by the hydroxyl group or by the carbonyl group followed by co-adsorption of MeOH. The most stable structures for this adsorption mode are ads_AA(C=O)-coads_MeOH and ads_AA(OH)-coads_MeOH. The second option (stepwise process) involves first MeOH adsorption on Brønsted acid site followed co-adsorption of AA (by C=O or OH group). In the third option, AA and MeOH adsorption on the BAS both occur simultaneously in a single step, sharing the proton of the zeolite (concerted process). We will only discuss in detail the most stable species that are shown in Fig. 5, with their respective energies in Table 1 and Fig. 6.

Stepwise process: in this case, the first molecule is adsorbed on the BAS and the next step involves the co-adsorption of the second molecule onto the adsorbed complex. It can be observed that adsorption of ads_AA(C=O) in the first single step (-143.7 kJ mol^{-1}) is energetically preferred than ads_MeOH or ads_AA(OH) adsorption (-130.7 and -79.6 kJ mol^{-1} respectively). Then, the second step should involve co-adsorption of the second adsorbate on the ads_AA(C=O) complex and, structures involving

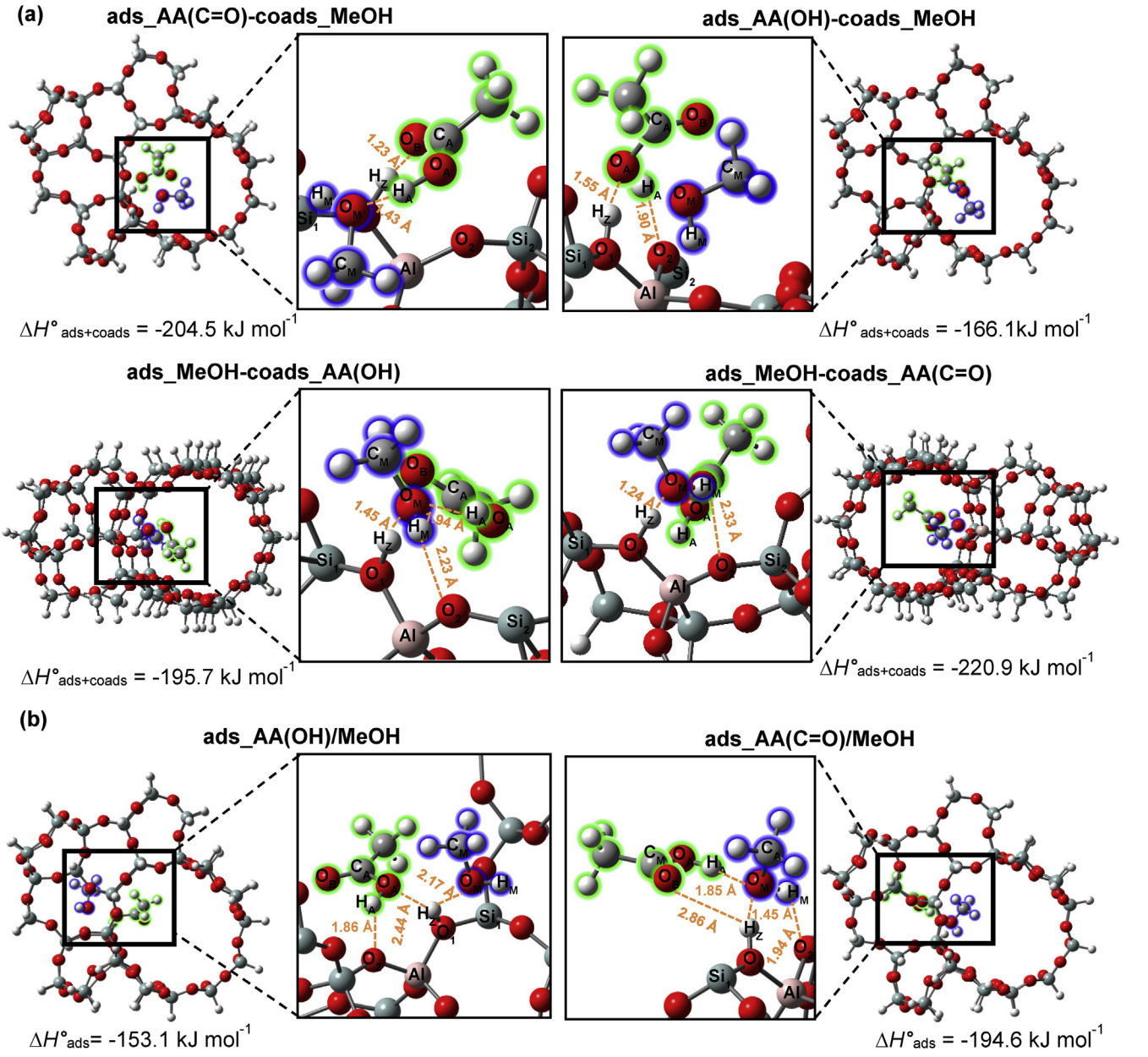

Fig. 5. Most stable structures found for adsorption of acetic acid/methanol complexes on H-Beta zeolite. (a) Stepwise process: adsorption of AA on BAS by carbonyl group and co-adsorption of MeOH, [ads_AA(C=O)-coads_MeOH]; adsorption of the AA on BAS by hydroxyl group and co-adsorption of MeOH, [ads_AA(OH)-coads_MeOH]; adsorption of MeOH on BAS and co-adsorption of AA by carbonyl group, [ads_MeOH-coads_AA(C=O)]; and adsorption of MeOH on BAS and co-adsorption of AA by hydroxyl group, [ads_MeOH-coads_AA(C=O)]. (b) Concerted process: adsorption of both AA by carbonyl group and MeOH on BAS, [ads_AA(C=O)/MeOH]; and adsorption of both AA by hydroxyl group and MeOH on BAS, [ads_AA(OH)/MeOH].

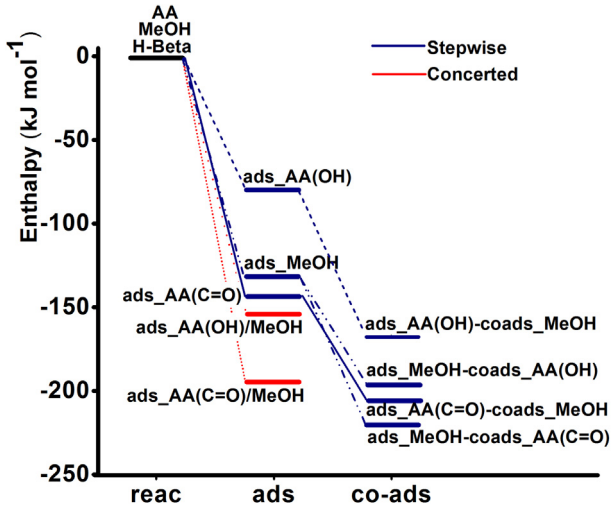

Fig. 6. Enthalpy profile for the adsorption and co-adsorption of methanol and acetic acid on H-Beta zeolite.

co-adsorption on the ads_MeOH or ads_AA(OH) complexes should be discarded according to energetic criteria (See Fig. 6).

As stated above, the most favorable complex involves the adsorption of AA by the carbonyl group on the BAS ($H_Z\cdots O_B$ = 1.23 Å) followed by co-adsorption of MeOH ($H_A\cdots O_M$ = 1.43 Å), denoted as ads_AA(C=O)-coads_MeOH (the total energy complex, $\Delta H^\circ_{ads+coads} = -204.5$ kJ mol^{-1}). Computed bond distances for the main interactions suggest strong hydrogen bonding. In addition, ads_AA(OH)-coads_MeOH complex is found about 38.1 kJ mol^{-1} higher in energy. In the last complex, AA binds to the Brønsted site by forming two hydrogen bonds, $H_Z\cdots O_A$ and $H_A\cdots O_2$, with the bond distances of 1.55 Å and 1.90 Å respectively, while the MeOH interacts with the methyl group of adsorbed AA by a weak interaction (dC-H$\cdots O_M$ = 2.42 Å). It is interesting to point out that this last complex higher in energy, corresponds to a structure according to Scheme 4 of proposed mechanism in the article published by Bedard and co-workers [23]. However, according to our results is more favorable a co-adsorbed complex where AA interacts with the BAS by the carbonyl group.

For the ads_MeOH-coads_AA(C=O) or ads_MeOH-coads_AA(OH) complexes, the MeOH is first adsorbed on BAS, followed by the AA co-adsorption. For ads_MeOH-coads_AA(C=O), there is a strong adsorption of MeOH on BAS ($dH_z\cdots O_M$ = 1.24 Å) and the AA binds to the MeOH ($dO_B\cdots H_M$ = 1.98 Å) without interacting directly with the active site. For the ads_MeOH-coads_AA(OH) complex the $H_z\cdots O_M$ and $H_M\cdots O_2$ distances lie in 1.45 Å and 2.23 Å respectively, and the $H_A\cdots O_M$ distance lies in the 1.94 Å value.

Concerted process: for adsorption of both AA and MeOH on BAS, the results show that ads_AA(C=O)/MeOH is the most stable complex, with a total enthalpy of −194.6 kJ mol^{-1}. If we considered the dimer AA/M-OH adsorbed complex of the postulated mechanism of Bedard [23] where the adsorption of AA takes place through the hydroxyl group, the ads_AA(OH)/MeOH complex is formed. However, again we found that the ads_AA(C=O)/MeOH complex that involves adsorption of both AA by carbonyl group and MeOH on BAS is preferred by 41.5 kJ mol^{-1} (ΔH°_{ads} = −194.6 vs −153.1 kJ mol^{-1}).

Concerning the most stable structure, an interesting feature is that the proton of Brønsted acid site (H_z) is shared between the two adsorbed molecules and, MeOH also interacts with one of the neighboring basic oxygen atom of the zeolite (O_2); in addition, there is a guest-guest interaction between AA and MeOH. For the other complex, AA interacts by the hydroxyl group with the acid and basic site of zeolite (similarly to the structure of the stepwise adsorption mechanism; however, longer distances are observed) and, the two adsorbed molecules share the H_z proton. A similar feature was observed for the other complex, where the hydroxyl groups of both AA and MeOH share the H_z proton of the zeolite.

Stepwise vs concerted: In addition to ads_AA(C=O)/coads_MeOH co-adsorption complex, AA/MeOH dimer complexes may also form at the Brønsted acid site. Hence, AA/MeOH dimer formation may compete with the formation of co-adsorbed complexes. It can be observed that adsorption of AA (by carbonyl group) and MeOH in a single step (−194.6 kJ mol^{-1}) is energetically preferred than AA (−143.7 kJ mol^{-1}) or MeOH (−130.7 kJ mol^{-1}) adsorption, and then the adsorption of both reactants in the concerted way will be the energetically favored process (See Fig. 6). Additionally, the ads_AA(C=O)-coads_MeOH co-adsorbed complex is most stable than the ads_AA(C=O)/MeOH dimer complex by about 9.9 kJ mol^{-1}. However, it should be emphasized that the interaction energy between differences are small.

Summing up, the results provide evidence that formation of the AA/MeOH adsorbed complex on a Brønsted acid site can originate from two separate pathways, giving rise to different adsorption structures. In one pathway, the dimer adsorption complex is formed by adsorbing one AA (by C=O or by OH group) or MeOH molecule at a time on the adsorption site followed by the co-adsorption of the second molecule in a stepwise process. In the other pathway, the AA/MeOH adsorbed complex is formed by the simultaneous adsorption of both AA and MeOH on a single Brønsted acid site in a concerted process. Considering the most stable structures from both pathways, there are no significant differences when comparing the magnitudes of the energy between ads_AA(C=O)-coads_MeOH and ads_AA(C=O)/MeOH adsorbed complexes.

In any case, the above results do not change the general picture commented above: the complexes where the AA is adsorbed by the carbonyl group are clearly the most stable ones. Thus, the rate-determining reaction step should involve these adsorbed complexes where acetic acid interacts with the zeolite by carbonyl group, and then the mechanism should involve the protonation of

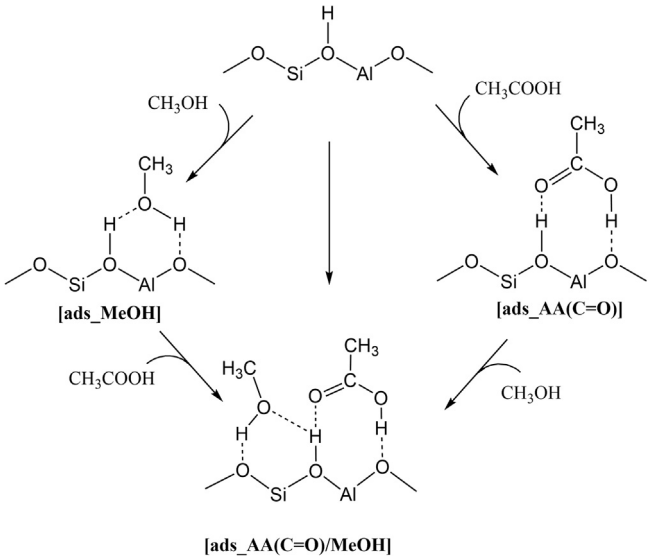

Scheme 2. Revised mechanism for the formation of the adsorbed complex of acetic acid/methanol.

the carbonyl group of acetic acid or the methanol molecule or otherwise methanol and AA(C=O) are adsorbed on a single acid site and react in a single concerted step. The revised mechanism for the formation of the adsorbed complex of acetic acid/methanol is shown in Scheme 2.

4. Conclusions

In this work, TGA-IR, ATR-FTIR and DFT calculations at M06–2X/6-31G(D) level are used for studying the adsorption of acetic acid and methanol on H-Beta zeolite as a model of reaction of the first step of esterification of FFA on H-zeolites in order to gain a deeper understanding of the adsorption mechanism of these chemical reactions.

Experimental results by coupled TGA-IR indicate different adsorption processes on H-Beta, which are simultaneous for both reagents and identify the ideal molecular adsorption range between 50 °C and 206 °C for MeOH and between 90 °C and 250 °C for AA. These results suggest that the first process observed on the DTG curve for both thermogravimetric experiments is related to the evolution of MeOH and AA bands monitored by IR. The evolved gas analysis clearly demonstrate that there is evolution of these species without any reaction at temperatures below 250 °C for AA and 206 °C for MeOH. The substrates are physisorbed on these temperature ranges due to the strong hydrogen interactions between them and the catalyst.

The adsorption of methanol on H-Beta is characterized by ν(C-H) stretching bands at 2956 cm^{-1} and 2847 cm^{-1} and by ν(OH) that decreases drastically in intensity after adsorption, showing a physical adsorption. Spectroscopic analysis of acetic acid adsorption shows vibrational bands corresponding to νC=O and δCH_3 modes, and another vibrational band centered at 3122 cm^{-1} in the experimental spectrum. The last one is assigned to OH stretching frequency in the ads_AA(C=O) complex, according to the calculated frequencies. This vibrational frequency is associated with the OH stretching of the acetic acid toward the Al-O-Si bridge of the zeolite, indicating that the adsorption mode of acetic acid is related to the adsorption of the carbonyl group on the Brønsted acid site. Thus, the predominant adsorption mode involves the ads_AA(C=O) complex where the acetic acid is molecularly adsorbed by the carbonyl group on the Brønsted acid site of catalyst, and the OH group is oriented to the Al-O-Si bridge.

Additionally, DFT calculations are utilized to predict and identify the adsorption pathways of both species, since it has been suggested by other authors that both AA and alcohol are involved in the rate-determining step for esterification reactions on zeolites. From the theoretical viewpoint, different models of adsorption of acetic acid and methanol on the surface of H-Beta zeolite were studied. The results found in the present work show that there are two possible adsorption pathways, namely the stepwise process where only one molecule interacts strongly with the BAS followed by weakly co-adsorption of the other molecule and, the concerted process where both acetic acid and methanol molecules interact with the acid site. Both adsorption pathways predict that the acetic acid is adsorbed by the carbonyl group, and the most stable species involved a dimer of acetic acid/methanol adsorbed on the Brønsted acid site.

Acknowledgements

The authors acknowledge to Agencia Nacional de Promoción Científica y Tecnológica (grant FONCYT-PICT-0465), Secretaría de Ciencia y Tecnología de la Universidad Nacional del Nordeste (grant F017-2014 SECYT-UNNE), and Consejo Nacional de Investigaciones Científicas y Técnicas (grant PIP-00678 CONICET) of Argentina, and Coordenação de Aperfeiçoamento de Pessoal de Nível Superior of Brazil for financial support. The authors also acknowledge the use of CPUs from the High Performance Computing Center of the Northeastern of Argentina (CECONEA) and Zeolyst International for providing the catalyst.

Appendix A. Supplementary data

Supplementary data related to this article can be found at http://dx.doi.org/10.1016/j.micromeso.2017.06.008.

References

[1] M. Harvey, S. Pilgrim, The new competition for land: food, energy, and climate change, Food Policy 36 (Supplement 1) (2011) S40–S51.
[2] T. Ennaert, J. Van Aelst, J. Dijkmans, R. De Clercq, W. Schutyser, M. Dusselier, D. Verboekend, B.F. Sels, Potential and challenges of zeolite chemistry in the catalytic conversion of biomass, Chem. Soc. Rev. 45 (2016) 584–611.
[3] T.A. Peters, N.E. Benes, A. Holmen, J.T.F. Keurentjes, Comparison of commercial solid acid catalysts for the esterification of acetic acid with butanol, Appl. Catal. A Gen. 297 (2006) 182–188.
[4] A.F. Lee, J.A. Bennett, J.C. Manayil, K. Wilson, Heterogeneous catalysis for sustainable biodiesel production via esterification and transesterification, Chem. Soc. Rev. 43 (2014) 7887–7916.
[5] M. Milina, S. Mitchell, J. Pérez-Ramírez, Prospectives for bio-oil upgrading via esterification over zeolite catalysts, Catal. Today 235 (2014) 176–183.
[6] L. Ciddor, J.A. Bennett, J.A. Hunns, K. Wilson, A.F. Lee, Catalytic upgrading of bio-oils by esterification, J. Chem. Technol. Biotechnol. 90 (2015) 780–795.
[7] L.J. Konwar, R. Das, A.J. Thakur, E. Salminen, P. Mäki-Arvela, N. Kumar, J.-P. Mikkola, D. Deka, Biodiesel production from acid oils using sulfonated carbon catalyst derived from oil-cake waste, J. Mol. Catal. A Chem. 388–389 (2014) 167–176.
[8] D.A.G. Aranda, J.d.A. Gonçalves, J.S. Peres, A.L.D. Ramos, C.A.R. de Melo, O.A.C. Antunes, N.C. Furtado, C.A. Taft, The use of acids, niobium oxide, and zeolite catalysts for esterification reactions, J. Phys. Org. Chem. 22 (2009) 709–716.
[9] K. Suwannakarn, E. Lotero, J.G. Goodwin, A comparative study of gas phase esterification on solid acid catalysts, Catal. Lett. 114 (2007) 122–128.
[10] R. Purova, K. Narasimharao, N.S.I. Ahmed, S. Al-Thabaiti, A. Al-Shehri, M. Mokhtar, W. Schwieger, Pillared HMCM-36 zeolite catalyst for biodiesel production by esterification of palmitic acid, J. Mol. Catal. A Chem. 406 (2015) 159–167.
[11] A. Palani, A. Pandurangan, Esterification of terephthalic acid with methanol over mesoporous Al-MCM-41 molecular sieves, J. Mol. Catal. A Chem. 245 (2006) 101–105.
[12] A. Corma, State of the art and future challenges of zeolites as catalysts, J. Catal. 216 (2003) 298–312.
[13] K.-H. Chung, B.-G. Park, Esterification of oleic acid in soybean oil on zeolite catalysts with different acidity, J. Ind. Eng. Chem. 15 (2009) 388–392.
[14] S.S. Vieira, Z.M. Magriotis, N.A.V. Santos, A.A. Saczk, C.E. Hori, P.A. Arroyo, Biodiesel production by free fatty acid esterification using lanthanum (La3+) and HZSM-5 based catalysts, Bioresour. Technol. 133 (2013) 248–255.
[15] A.A. Costa, P.R.S. Braga, J.L. de Macedo, J.A. Dias, S.C.L. Dias, Structural effects of WO3 incorporation on USY zeolite and application to free fatty acids esterification, Microporous Mesoporous Mat. 147 (2012) 142–148.
[16] S.S. Vieira, Z.M. Magriotis, M.F. Ribeiro, I. Graça, A. Fernandes, J.M.F.M. Lopes, S.M. Coelho, N.A.V. Santos, A.A. Saczk, Use of HZSM-5 modified with citric acid as acid heterogeneous catalyst for biodiesel production via esterification of oleic acid, Microporous Mesoporous Mat. 201 (2015) 160–168.
[17] S.S. Vieira, Z.M. Magriotis, I. Graça, A. Fernandes, M.F. Ribeiro, J.M.F.M. Lopes, S.M. Coelho, N.A.V. Santos, A.A. Saczk, Production of biodiesel using HZSM-5 zeolites modified with citric acid and SO42−/La2O3, Catal. Today 279 (Part 2) (2017) 267–273.
[18] D.R. Fernandes, A.S. Rocha, E.F. Mai, C.J.A. Mota, V. Teixeira da Silva, Levulinic acid esterification with ethanol to ethyl levulinate production over solid acid catalysts, Appl. Catal. A Gen. 425–426 (2012) 199–204.
[19] E. Lotero, Y. Liu, D.E. Lopez, K. Suwannakarn, D.A. Bruce, J.G. Goodwin, Synthesis of biodiesel via acid catalysis, Ind. Eng. Chem. Res. 44 (2005) 5353–5363.
[20] G. Perot, M. Guisnet, Advantages and disadvantages of zeolites as catalysts in organic chemistry, J. Mol. Catal. 61 (1990) 173–196.
[21] H.M. Koo, J.H. Lee, T.-S. Chang, Y.-W. Suh, D.H. Lee, J.W. Bae, Esterification of acetic acid with methanol to methyl acetate on Pd-modified zeolites: effect of Brønsted acid site strength on activity, Reac. Kinet. Mech. Catal. 112 (2014) 499–510.
[22] K.-H. Chung, D.-R. Chang, B.-G. Park, Removal of free fatty acid in waste frying oil by esterification with methanol on zeolite catalysts, Bioresour. Technol. 99 (2008) 7438–7443.
[23] J. Bedard, H. Chiang, A. Bhan, Kinetics and mechanism of acetic acid esterification with ethanol on zeolites, J. Catal. 290 (2012) 210–219.

[24] J.K. Satyarthi, S. Radhakrishnan, D. Srinivas, Factors influencing the kinetics of esterification of fatty acids over solid acid catalysts, Energy fuels. 25 (2011) 4106–4112.
[25] R. Koster, B. van der Linden, E. Poels, A. Bliek, The mechanism of the gas-phase esterification of acetic acid and ethanol over MCM-41, J. Catal. 204 (2001) 333–338.
[26] S.R. Kirumakki, N. Nagaraju, K.V.R. Chary, Esterification of alcohols with acetic acid over zeolites Hβ, HY and HZSM5, Appl. Catal. A Gen. 299 (2006) 185–192.
[27] J. Van der Mynsbrugge, K. Hemelsoet, M. Vandichel, M. Waroquier, V. Van Speybroeck, Efficient approach for the computational study of alcohol and nitrile adsorption in H-ZSM-5, J. Phys. Chem. C 116 (2012) 5499–5508.
[28] A. Corma, Heterogeneous catalysis: understanding for designing, and designing for applications, Angew. Chem. Int. Ed. 55 (2016) 6112–6113.
[29] M.F. Zalazar, D.J.R. Duarte, N.M. Peruchena, Adsorption of alkenes on acidic zeolites. Theoretical study based on the electron charge density, J. Phys. Chem. A 113 (2009) 13797–13807.
[30] M.F. Zalazar, N.M. Peruchena, Topological analysis of the electronic charge density in the ethene protonation reaction catalyzed by acidic zeolite, J. Phys. Chem. A 111 (2007) 7848–7859.
[31] M.F. Zalazar, N.M. Peruchena, Topological description of the bond breaking and bond forming processes of the alkene protonation reaction in the zeolite chemistry: an AIM study, J. Mol. Model. 17 (2011) 2501–2511.
[32] M.F. Zalazar, N. Peruchena, Laplacian of the electron density: a hole-lump interaction as a tool to study stereoelectronic control of chemical reactions, J. Phys. Org. Chem. 27 (2014) 327–335.
[33] S. Brunauer, P.H. Emmett, E. Teller, Adsorption of gases in multimolecular layers, J. Am. Chem. Soc. 60 (1938) 309–319.
[34] C. Baerlocher, L.B. McCusker, Database of Zeolite Structures, International Zeolite Association.
[35] D. Lesthaeghe, B. De Sterck, V. Van Speybroeck, G.B. Marin, M. Waroquier, Zeolite shape-selectivity in the gem-methylation of aromatic hydrocarbons, Angew. Chem. Int. Ed. 46 (2007) 1311–1314.
[36] H. Fang, A. Zheng, J. Xu, S. Li, Y. Chu, L. Chen, F. Deng, Theoretical investigation of the effects of the zeolite framework on the stability of carbenium ions, J. Phys. Chem. C 115 (2011) 7429–7439.
[37] J. Van der Mynsbrugge, M. Visur, U. Olsbye, P. Beato, M. Bjørgen, V. Van Speybroeck, S. Svelle, Methylation of benzene by methanol: single-site kinetics over H-ZSM-5 and H-beta zeolite catalysts, J. Catal. 292 (2012) 201–212.
[38] R.E. Patet, S. Caratzoulas, D.G. Vlachos, Adsorption in zeolites using mechanically embedded ONIOM clusters, Phys. Chem. Chem. Phys. 18 (2016) 26094–26106.
[39] Y. Zhao, D.G. Truhlar, The Minnesota density functionals and their applications to problems in mineralogy and geochemistry, Rev. Mineral. Geochem. 71 (2010) 19–37.
[40] Y. Zhao, D.G. Truhlar, Benchmark data for interactions in zeolite model complexes and their use for assessment and validation of electronic structure methods, J. Phys. Chem. C 112 (2008) 6860–6868.
[41] T. Maihom, B. Boekfa, J. Sirijaraensre, T. Nanok, M. Probst, J. Limtrakul, Reaction mechanisms of the methylation of ethene with methanol and dimethyl ether over H-ZSM-5: an ONIOM study, J. Phys. Chem. C 113 (2009) 6654–6662.
[42] K. Kongpatpanich, T. Nanok, B. Boekfa, M. Probst, J. Limtrakul, Structures and reaction mechanisms of glycerol dehydration over H-ZSM-5 zeolite: a density functional theory study, Phys. Chem. Chem. Phys. 13 (2011) 6462–6470.
[43] T. Maihom, P. Pantu, C. Tachakritikul, M. Probst, J. Limtrakul, Effect of the zeolite nanocavity on the reaction mechanism of n-Hexane cracking: a density functional theory study, J. Phys. Chem. C 114 (2010) 7850–7856.
[44] P. Charoenwiangnuea, T. Maihom, P. Kongpracha, J. Sirijaraensre, J. Limtrakul, Adsorption and decarbonylation of furfural over H-ZSM-5 zeolite: a DFT study, RSC Adv. 6 (2016) 105888–105894.
[45] J. Gomes, P.M. Zimmerman, M. Head-Gordon, A.T. Bell, Accurate prediction of hydrocarbon interactions with zeolites utilizing improved exchange-correlation functionals and QM/MM methods: benchmark calculations of adsorption enthalpies and application to ethene methylation by methanol, J. Phys. Chem. C 116 (2012) 15406–15414.
[46] M.K. Kesharwani, B. Brauer, J.M.L. Martin, Frequency and zero-point vibrational energy scale factors for double-Hybrid density functionals (and other selected methods): can anharmonic force fields Be avoided? J. Phys. Chem. A 119 (2015) 1701–1714.
[47] M.J. Frisch, G.W. Trucks, H.B. Schlegel, G.E. Scuseria, M.A. Robb, J.R. Cheeseman, J.A. Montgomery, T. Vreven, K.N. Kudin, J.C. Burant, J.M. Millam, S.S. Iyengar, J. Tomasi, V. Barone, B. Mennucci, M. Cossi, G. Scalmani, N. Rega, G.A. Petersson, H. Nakatsuji, M. Hada, M. Ehara, K. Toyota, R. Fukuda, J. Hasegawa, M. Ishida, T. Nakajima, Y. Honda, O. Kitao, H. Nakai, M. Klene, X. Li, J.E. Knox, H.P. Hratchian, J.B. Cross, C. Adamo, J. Jaramillo, R. Gomperts, R.E. Stratmann, O. Yazyev, A.J. Austin, R. Cammi, C. Pomelli, J.W. Ochterski, P.Y. Ayala, K. Morokuma, G.A. Voth, P. Salvador, J.J. Dannenberg, G. Zakrzewski, S. Dapprich, A.D. Daniels, M.C. Strain, O. Farkas, D.K. Malick, A.D. Rabuck, K. Raghavachari, J.B. Foresman, J.V. Ortiz, Q. Cui, A.G. Baboul, S. Clifford, J. Cioslowski, B.B. Stefanov, G. Liu, A. Liashenko, P. Piskorz, I. Komaromi, R.L. Martin, D.J. Fox, T. Keith, M.A. Al-Laham, C.Y. Peng, A. Nanayakkara, M. Challacombe, P.M.W. Gill, B. Johnson, W. Chen, M.W. Wong, C. Gonzalez, J.A. Pople, Gaussian 09, Gaussian, Inc., Wallingford, CT, 2009.
[48] G.D. Knowlton, T.R. White, H.L. McKague, Thermal study of types of water associated with clinoptilolite, Clays Clay Min. 29 (1981) 403–411.
[49] Y. Wei, Y. He, D. Zhang, L. Xu, S. Meng, Z. Liu, B.-L. Su, Study of Mn incorporation into SAPO framework: synthesis, characterization and catalysis in chloromethane conversion to light olefins, Microporous Mesoporous Mat. 90 (2006) 188–197.
[50] M. Hippler, S. Hesse, M.A. Suhm, Quantum-chemical study and FTIR jet spectroscopy of CHCl3-NH3 association in the gas phase, Phys. Chem. Chem. Phys. 12 (2010) 13555–13565.
[51] C. Busco, A. Barbaglia, M. Broyer, V. Bolis, G.M. Foddanu, P. Ugliengo, Characterisation of Lewis and Brønsted acidic sites in H-MFI and H-BEA zeolites: a thermodynamic and ab initio study, Thermochim. Acta 418 (2004) 3–9.
[52] S. Bordiga, C. Lamberti, F. Bonino, A. Travert, F. Thibault-Starzyk, Probing zeolites by vibrational spectroscopies, Chem. Soc. Rev. 44 (2015) 7262–7341.
[53] A. Zecchina, G. Spoto, S. Bordiga, Probing the acid sites in confined spaces of microporous materials by vibrational spectroscopy, Phys. Chem. Chem. Phys. 7 (2005) 1627–1642.
[54] G. Mirth, J.A. Lercher, Surface chemistry of methanol on HZSM5, Stud. Surf. Sci. Catal. 61 (1991) 437–443.
[55] B. Hunger, S. Matysik, M. Heuchel, W.-D. Einicke, Adsorption of water and methanol on a NaZSM-5 zeolite. A temperature-programmed desorption (TPD) study, J. Therm. Anal. Calorim. 64 (2001) 1183–1190.
[56] R.M. Silverstein, F.X. Webster, D.J. Kiemle, D.L. Bryce, Spectrometric Identification of Organic Compounds, eighth ed., John Wiley & Sons, 2015.
[57] L. Kubelková, J. Nováková, K. Nedomová, Reactivity of surface species on zeolites in methanol conversion, J. Catal. 124 (1990) 441–450.
[58] O. Kresnawahjuesa, R.J. Gorte, D. White, Characterization of acylating intermediates formed on H-ZSM-5, J. Mol. Catal. A Chem. 208 (2004) 175–185.
[59] T.K. Phung, A.A. Casazza, B. Aliakbarian, E. Finocchio, P. Perego, G. Busca, Catalytic conversion of ethyl acetate and acetic acid on alumina as models of vegetable oils conversion to biofuels, Chem. Eng. J. 215–216 (2013) 838–848.
[60] L.M. Parker, Sorption of acetic acid on H+ZSM-S, Stud. Surf. Sci. Catal. 36 (1988) 589–595.
[61] R.J. Gorte, Design parameters for temperature programmed desorption from porous catalysts, J. Catal. 75 (1982) 164–174.
[62] E.M.S. Maçôas, L. Khriachtchev, M. Pettersson, R. Fausto, M. Räsänen, Rotational isomerism in acetic Acid: the first experimental observation of the high-energy conformer, J. Am. Chem. Soc. 125 (2003) 16188–16189.
[63] S. Svelle, C. Tuma, X. Rozanska, T. Kerber, J. Sauer, Quantum chemical modeling of zeolite-catalyzed methylation reactions: toward chemical accuracy for barriers, J. Am. Chem. Soc. 131 (2009) 816–825.
[64] C.M. Nguyen, M.-F. Reyniers, G.B. Marin, Theoretical study of the adsorption of C1-C4 primary alcohols in H-ZSM-5, Phys. Chem. Chem. Phys. 12 (2010) 9481–9493.
[65] K. Stückenschneider, J. Merz, G. Schembecker, Molecular interactions of alcohols with zeolite BEA and MOR frameworks, J. Mol. Model. 19 (2013) 5611–5624.
[66] A. Zecchina, S. Bordiga, G. Spoto, D. Scarano, G. Spano, F. Geobaldo, IR spectroscopy of neutral and ionic hydrogen-bonded complexes formed upon interaction of CH3OH, C2H5OH, (CH3)2O, (C2H5)2O and C4H8O with H-Y, H-ZSM-5 and H-mordenite: comparison with analogous adducts formed on the H-Nafion superacidic membrane, J. Chem. Soc. Faraday Trans. 92 (1996) 4863–4875.
[67] J. Kotrla, D. Nachtigallová, L. Kubelková, L. Heeribout, C. Doremieux-Morin, J. Fraissard, Hydrogen bonding of methanol with bridged OH groups of Zeolites: ab initio calculation, 1H NMR and FTIR studies, J. Phys. Chem. B 102 (1998) 2454–2463.
[68] G. Mirth, J.A. Lercher, M.W. Anderson, J. Klinowski, Adsorption complexes of methanol on zeolite ZSM-5, J. Chem. Soc. Faraday Trans. 86 (1990) 3039–3044.
[69] C. Pazé, S. Bordiga, C. Lamberti, M. Salvalaggio, A. Zecchina, G. Bellussi, Acidic properties of H–β zeolite as probed by bases with proton affinity in the 118–204 kcal mol-1 Range: a FTIR investigation, J. Phys. Chem. B 101 (1997) 4740–4751.
[70] F. Haase, J. Sauer, Interaction of methanol with Brönsted acid sites of zeolite catalysts: an ab initio study, J. Am. Chem. Soc. 117 (1995) 3780–3789.
[71] C.M. Nguyen, M.-F. Reyniers, G.B. Marin, Adsorption thermodynamics of C1–C4 alcohols in H-FAU, H-MOR, H-ZSM-5, and H-ZSM-22, J. Catal. 322 (2015) 91–103.
[72] I. Doroshenko, V. Pogorelov, V. Sablinskas, V. Balevicius, Matrix-isolation study of cluster formation in methanol: O–H stretching region, J. Mol. Liq. 157 (2010) 142–145.
[73] K. Alexopoulos, M.-S. Lee, Y. Liu, Y. Zhi, Y. Liu, M.-F. Reyniers, G.B. Marin, V.-A. Glezakou, R. Rousseau, J.A. Lercher, Anharmonicity and confinement in zeolites: structure, spectroscopy, and adsorption free energy of ethanol in H-ZSM-5, J. Phys. Chem. C 120 (2016) 7172–7182.
[74] C.C. Lee, R.J. Gorte, W.E. Farneth, Calorimetric study of alcohol and nitrile adsorption complexes in H-ZSM-5, J. Phys. Chem. B 101 (1997) 3811–3817.
[75] T. Steiner, The hydrogen bond in the solid state, Angew. Chem. Int. Ed. 41 (2002) 48–76.
[76] B. Murphy, M.E. Davis, B. Xu, The effect of adsorbed molecule gas-phase deprotonation enthalpy on ion exchange in sodium exchanged zeolites: an in situ FTIR investigation, Top. Catal. 58 (2015) 393–404.